Chapter VI

Effect of Cetyltrimethylammonium bromide on the aggregation behaviour of Sodiumdodecylbenzene sulfonate

Chapter VI

Effect of cetyltrimethylammonium bromide on the aggregation behaviour of Sodiumdodecylbenzene sulfonate

6.1 Introduction and review of the previous work

Molecular self-assembly provides a powerful tool for the creation of well-organized structures in the nanometre or micrometer length scale, such as micelles, vesicles, fibres, discs and tubes [1 - 6]. Conventional micelles are fluid aggregates of surfactants with shape and size, controlled by packing of individual surfactants. The main characteristics of such micelles are: (a) These micelles, especially the charged micelles, are stabilized by hydrophobic forces and head group repulsions (electrostatic and steric), (b) Each surfactant moves as in a fluid and the size and shape and aggregation numbers are decided by the packing parameter as mentioned above, (c) Length scales of these micelles are in 10 - 1000 Å (d) The life times of these micelles are often in milliseconds. On dilution below critical micelle concentration the aggregates disappear in milliseconds. The realization that there could be micelles and aggregates of different type is recent [7 - 8]. Surfactant solutions represent a well-documented class of self-assembled systems that can offer diverse organized structures [9 - 11]. Above the critical micelle concentration (cmc), hydrophilic surfactants form small globular micellar aggregates and the solutions show Newtonian flow behaviour. Compared to single surfactant, the mixed surfactant exhibits superior interfacial properties such as higher surface activity and lower critical micelle concentration (cmc). The mixtures of surfactants which have been studied include cationic/anionic, non ionic/non ionic, cationic/non ionic, anionic/non ionic, cationic/cationic etc. Surfactant mixtures are commonly preferred in medicinal and pharmaceutical formulations and industrial preparations due to the purpose of suspension, solubilization and dispersion. Ionic surfactants can also self assembled to long thread-like or worm-like micelles in presence of certain organic ions e.g., sodium salicylate. Under certain conditions such as concentration, salinity, temperature, presence of counterions, etc., the globular micelles may undergo uniaxial growth and form very

long and highly flexible aggregates, referred to as "wormlike" or "threadlike" micelles [12 - 19]. Wormlike micelles [13] are long, self-assembled, semi-flexible, breakable polymer-like materials with surfactant heads on the outside and tails in the core. They display a striking range of dynamical properties, including anomalous relaxation, shear banding, and rheological chaos [20, 21]. Due to this reason, wormlike micelles have received considerable attention from theoretician and experimentalist during the past few decades. Earlier, an extensive study on the dynamics and rheological behaviour of wormlike micelles began in long-chain ionic surfactant systems in the presence of a salt [22-25]. Above a threshold concentration c*, wormlike micelles may entangle into a transient network, which displays remarkable viscoelastic properties. The rheological behaviour observed for wormlike micelles in the surfactant solution is similar to that for flexible polymers, and therefore, aqueous solutions of entangled wormlike micelles are often called "living polymer systems". The research of wormlike micelles has drawn considerable interest owing to their superior properties and wide applications as has been already mentioned [26–29]. Viscoelastic wormlike micelles or threadlike micelles have been observed in various surfactant systems, including mixtures of cationic and anionic surfactants [30-32], nonionic surfactants [32–34], zwitterionic surfactants [35–37] and ionic surfactants with different activities [38–43]. Hydrotopes were also found to promote the formation of viscoelastic wormlike micelles in ionic surfactant solutions, in which the surfactant interact strongly with hydrotrope due to electrostatic attraction and hydrophobic effect. Salicylate, tosylate, chlorobenzoate, hydroxynaphthalenecarboxylates and nitrobenzoate (all containing an aromatic group) were reported to induce wormlike micelle formation in a cationic surfactant solution. Unlike surfactant molecules, hydrotropes are a class of amphiphilic compounds that cannot form well-organized structures, such as micelles, but do increase the solubility of organic molecules in water by several orders of magnitude. The common structural characteristics of hydrotropes are the coexistence of an unsaturated hydrocarbon ring and an ionic group within one molecule. Strong synergistic effects are often observed when hydrotropes are added to aqueous surfactants or polymer solutions. In particular, various hierarchically self-assembled structures such as tubes, ribbons, vesicles and lamellar structures can be fabricated in mixtures of surfactants and hydrotropes.

Mixtures of cationic and anionic surfactants show not only synergistic effect of the aggregation properties but also triggered micellar grow in one dimension to form

long worm-like micelles. A dramatic influence on the viscosity of wormlike micelles in aqueous solutions of CTAB was shown for *trans-ortho*-methoxycinnamic acid [44]. While some works in this field is available in the literature, report on the effect of the aggregation properties of SDBS and CTAB mixture is rare. In this chapter, the results of the study on their mixing behaviour, synergism, and one dimensional grow to worm-like micelles and rheological characteristics of this system are reported. Through this development it became clear that by mixing surfactants (hydrotropes) of opposite charges, cationic and anionic, but with varying chain lengths one can control the degree of precipitation of the surfactants to produce different supramolecular structures like vesicles and polymeric micelles [45]. The transition from one structure to another is also well known facts in recent studies. A temperature-induced vesicle to micelle transition has been observed in the system of a new cationic surfactant cetyltrimethylammonium 3-hydroxy naphthalene 2-carboxylate [8]. Some researchers have also shown that the vesicle-to-micelle transition occurs in this system at 45°C and is induced by melting of vesicle surfaces using calorimetry and conductivity measurements. At melting the ions are released from surfaces, giving a jump in conductivity at this point and if there are trapped ions in vesicles they are also released [46]. The vesicle to micelle transition in different systems has been characterized by several techniques like rheology, light scattering, NMR, fluorescence, small angle neutron scattering (SANS), etc. Present study is divided in two major parts. In the first part, the synergistic effect of the mixing of cetyltrimethylammonium bromide (CTAB, a cationic surfactant) with SDBS (an anionic surfactant) is studied under Newtonian flow regime. In the second part, the formation of viscoelastic worm-like micelles is examined and the rheological behavior of the system is investigated under non Newtonian flow regime.

6. 2. Theoretical models for analyzing mixing behaviour of surfactants

Ideal and non-ideal mixture models under Newtonian flow regime.

The process of assembling free surfactant monomers to generate aggregates is, of course, entropically unfavourable as the entropy of mixing surfactant and solvent molecules then decreases. This unfavourable change in entropy of mixing decreases

with increasing surfactant concentration, C_{surf} or, otherwise expressed, the chemical potential of free surfactant monomers increases with increasing C_{surf} and, when the chemical potential of the free monomers becomes equal to the corresponding quantity in the surfactant aggregates, the latter start to form. The surfactant concentration where aggregates start to appear is known as the cmc; above this concentration aggregates and free surfactant monomers coexists.

When two surfactants or a surfactant and cosurfactants are mixed, mixed aggregates are formed and the cmc becomes a function of the surfactant concentration. For a mixture of two different surfactants, the cmc has been observed to depend linearly on the composition of the micelles, i.e.

$$\boldsymbol{cmc\ (x_1) = x_1\ cmc_1 + \ (1 - x_1)\ cmc_2} \qquad (6.1)$$

where x_1 denotes the mole fraction of one of the surfactants in the aggregates, and cmc_1 and cmc_2 are the cmcs of pure surfactants 1 and 2 respectively. Surfactant systems for which the cmc is seen to obey equation 6.1 are often referred to as ideal surfactant mixtures. The overall mole fraction of surfactant 1 at the cmc equals

$$\boldsymbol{y_1 \equiv \frac{cmc_1^m}{(cmc_1^m + cmc_2^m)}} \qquad (6.2)$$

where cmc_1^m and cmc_2^m the free monomer concentrations of surfactant 1 and 2 at $cmc(x_1) = cmc_1^m + cmc_2^m$, since by definition, the amount of surfactant existing as free monomers is much larger than the amount of aggregated surfactant at cmc. As a result, we can also write,

$$\boldsymbol{\frac{1}{cmc\ (y_1)} = \frac{y_1}{cmc_1} + \frac{(1-y_1)}{cmc_2}} \qquad (6.3)$$

However, for a number of surfactant mixtures synergistic effects are important which means that the cmc deviates appreciably from the behaviour predicted by above equation [47]. To account for these synergistic effects it is customary to write

$$\boldsymbol{cmc\,(x_1) = x_1 f_1\,(x_1)\,cmc_1 + (1 - x_1) f_2\,(x_1)\,cmc_2} \qquad (6.4)$$

where, in accordance with the theory of regular mixtures, activity factor functions are introduced by setting

$$\boldsymbol{f_1\,(x_1) = \exp[(1 - x_1)^2\,\beta]} \qquad (6.5)$$

and

$$\boldsymbol{f_2\,(x_1) = \exp\,(x_1)^2\,\beta]} \qquad (6.6)$$

In analogy with the treatment of regular mixtures, β is mostly referred to as the interaction parameter, and its deviation from zero (and, consequently, the deviation of f_1 and f_2 from unity) is commonly assumed to results from specific interactions between the surfactant headgroups (discussed in further detail under results and discussion section).

Formation of worm-like micelles and the study of viscoelastic characteristics under non-Newtonian flow regime is an interesting field, which have also been investigated and reported in the present thesis. Different theoretical models have also been proposed for micelle–vesicle transition mainly in lipid-detergent mixtures. These molecular approaches model was on the concept of curvature elasticity of thin films [48–50]. These models can take into account the basic characteristics of these transitions, in particular the presence of a two-phase region consisting of coexisting

vesicles and micelles. A similar model has also been proposed for vesicle to micelle transition in cationic anionic mixtures and the key concept is shown in the figure below [51–52]. Cationic and anionic surfactants, in view of their strong interaction in polar region, form dimers and higher n-mers even at low concentrations.

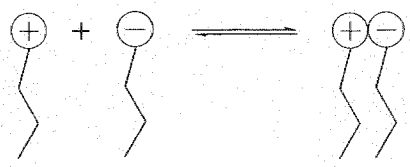

Figure 6.1: Strong coulomb interactions between the polar heads of cationic – anionic surfactants force them to form dimers, trimers, n-mers at interfaces of aggregates. Depending on the numbers, the bend elastic constant of the interface changes leading to formation of vesicles, worms, etc.

At any given temperature, these are in thermal equilibrium. The relative concentrations of these species decide whether the system forms worms, vesicles or crystals. The relative concentrations can be estimated from extensions of the concepts of Bjerrum transitions in two dimensions. Few of recent wide angle X- rays scattering studies have shown evidence to such melting of ion-pairs with temperature in cationic surfactant solutions [53].

5. 3 Experimental

Conductivity measurements were carried out on a Mettler Toledo digital conductometer (Model no. MC226), using a dip cell (specific conductance 1413 $S.cm^{-1}$). The experiments were performed at desired temperatures maintained within ± 0.5 K. Constant temperature was maintained by flowing water from the constant temperature water bath by an automatic motor to the double wall vessel containing the experimental solution. Surface tension was measured with a Kruss K9 tensiometer (Hamburg, Germany, accuracy ± 0.01 $mN.m^{-1}$) using the platinum ring detachment method. The temperature was controlled adopting the same arrangement as mentioned above. The surface tension was determined with a single measurement method. All measurements were repeated until the difference between two values was less than 0.2 mNm^{-1}. The rheological measurements were done using cone-plate

geometry with 4^0 truncation angle, with diameter 25 mm and 0.105 mm sample gap on a dynamic compact rheometer (Anton Paar, USA, Model MCR 302), equipped with Peltier temperature control system.

6.4. Preparation of solution of SDBS-CTAB mixed micelle system

A volume of 10 ml of water was taken in a beaker at room temperature (25°C) into which a stock solution of SDBS-CTAB mixed micelle system of desired concentration (4-6 times cmc) at the fixed composition was stepwise added with a micropipette as required. At each step of addition (concentration varies with every addition, the conductivity/surface tension was measured keeping the mole-fraction of SDBS and CTAB constant.

6. 5 Results and discussion

Micellar aggregates are also formed in an aqueous solution containing mixed surfactants. The cmc values obtained from the conductivity and surface tensiometry measurements are rendered in table 6.1. The individual cmc values of these two surfactants in pure water, measured by the above two techniques, are in agreement with the literature data.

Table 6.

Experimental cmc values of SDBS-CTAB mixed micelle system at different mol fractions of SDBS and CTAB measured by conductometrically and surface tensiometrically.

x_{SDBS}	x_{CTAB}	$cmc_{Conductance}$/ mM	$cmc_{Surface\ Tension}$ / mM
1.0	0.0	2.78	2.82
0.8	0.2	1.49	1.40
0.6	0.4	1.25	1.25
0.4	0.6	1.15	1.10
0.2	0.8	0.94	0.93
0.0	1.0	0.90	0.90

The plots for determination of cmc's (surface tension and conductometry) at different mole-fraction of CTAB and SDBS are shown in figure 6.2 to figure 6.13.

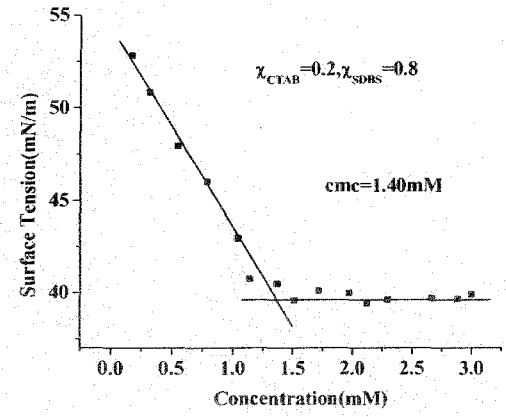

Figure 6.2: Surface tension vs. concentration plot at $\chi_{CTAB} = 0.2$; $\chi_{SDBS} = 0.8$.

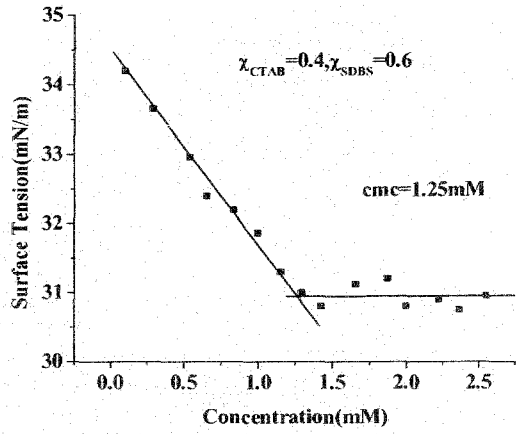

Figure 6.3: Surface tension vs. concentration plot at $\chi_{CTAB} = 0.4$; $\chi_{SDBS} = 0.6$.

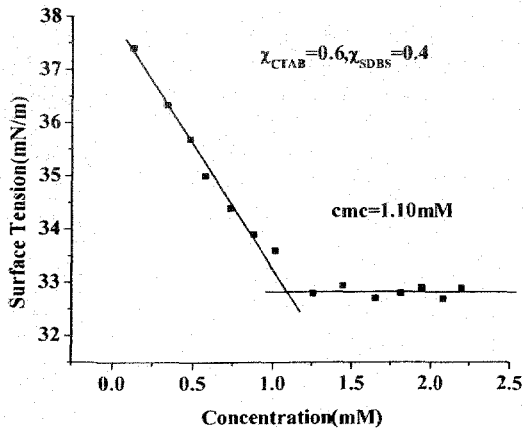

Figure 6.4: Surface tension vs. concentration plot at $\chi_{CTAB} = 0.6$; $\chi_{SDBS} = 0.4$.

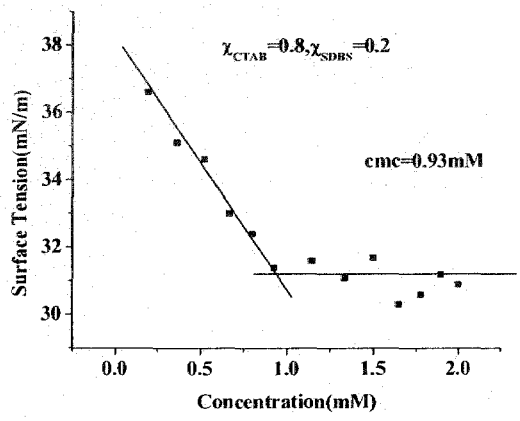

Figure 6.5: Surface tension vs. concentration plot at $\chi_{CTAB} = 0.8$; $\chi_{SDBS} = 0.2$.

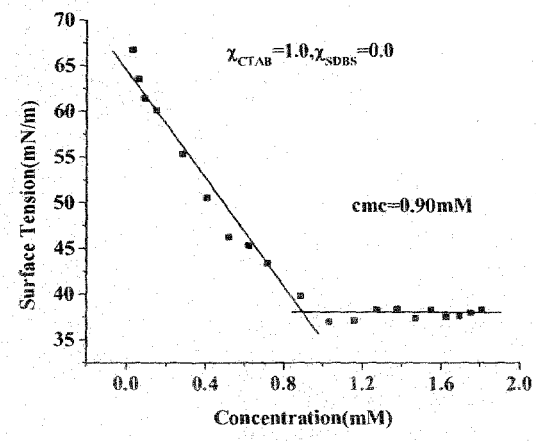

Figure 6.6: Surface tension vs. concentration plot at $\chi_{CTAB} = 1.0$; $\chi_{SDBS} = 0.0$.

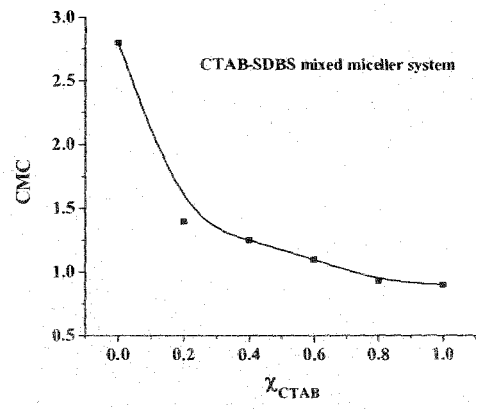

Figure 6.7: CTAB – SDBS mixed micelle system at different mol fraction and variation of cmc with mol fraction determined by surface tension method.

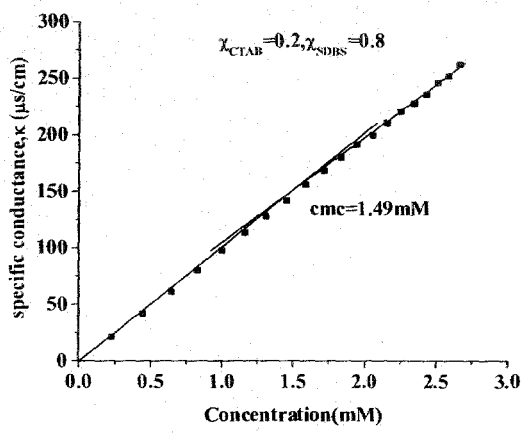

Figure 6.8: Conductance vs. concentration plot at $\chi_{CTAB} = 0.2$; $\chi_{SDBS} = 0.8$.

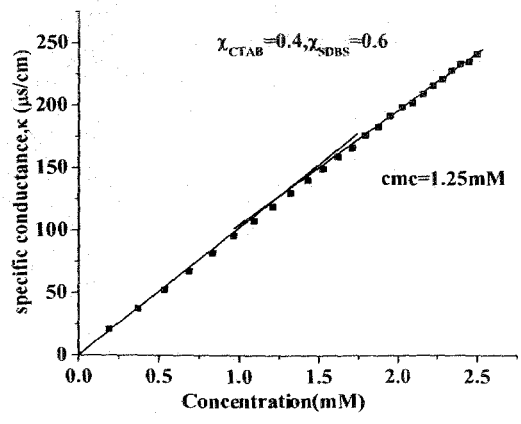

Figure 6.9: Conductance vs. concentration plot at $\chi_{CTAB} = 0.4$; $\chi_{SDBS} = 0.6$.

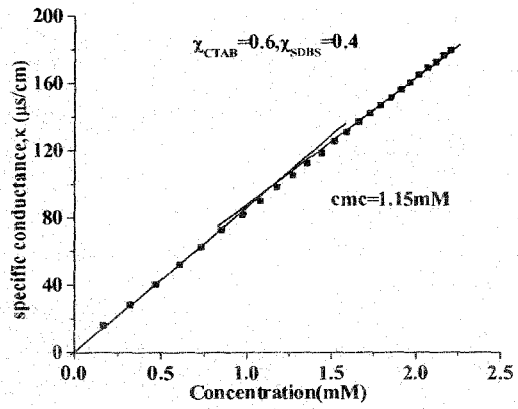

Figure 6.10: Conductance vs. concentration plot at $\chi_{CTAB} = 0.6$; $\chi_{SDBS} = 0.4$.

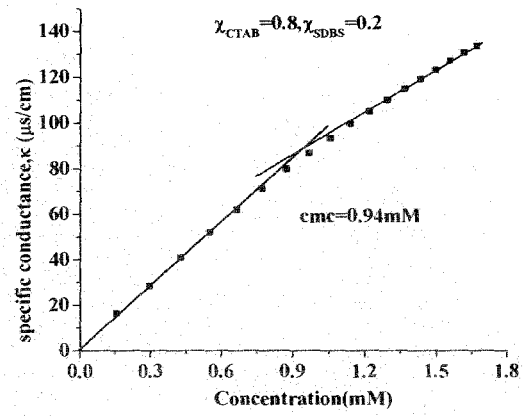

Figure 6.11: Conductance vs. concentration plot at $\chi_{CTAB} = 0.8$; $\chi_{SDBS} = 0.2$.

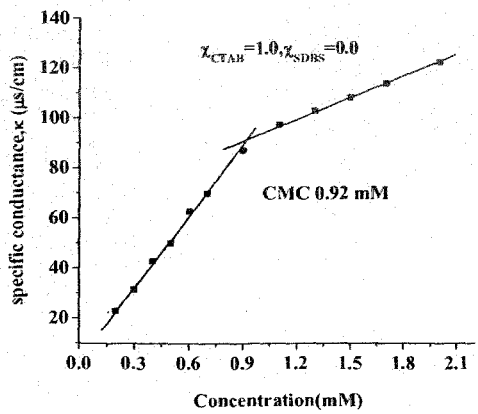

Figure 6.12: Conductance vs. concentration plot at $\chi_{CTAB} = 1.0$; $\chi_{SDBS} = 0.0$.

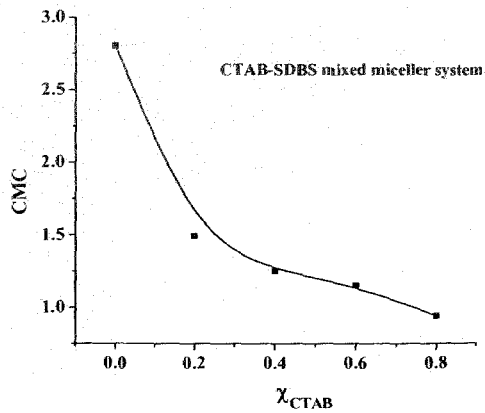

Figure 6.13: CTAB – SDBS mixed micelle system at different mol fraction and variation of cmc with mol fraction by conductivity method.

Here the cmc's were determined for the mixed surfactant systems of various mole ratios at a particular temperature. The break points in the surface tension vs. concentration or conductivity vs. concentration plots were taken as cmc. The values for CTAB and SDBS surfactants in pure water are in fair agreement with published data. Micellar aggregates are also formed in an aqueous solution containing SDBS and CTAB. But, the tendency of aggregation is different from that of the pure surfactants. Due to hydrophobic effect, the micellization process is a function of temperature, additive and solvent because the solvent property gets modified in the presence of an additive. However, the aggregation characteristic is found to be interesting because the cmc is a function of mole fraction of each component of the surfactant mixture. In general, the cmc values were found to decrease with the increase in mole fraction of the CTAB suggesting less ionic repulsive forces and stronger hydrophobic effect (figure 6.9 and 6.15). The results indicate that the added cationic surfactant (CTAB in this experiment) is assisting in the micelle formation of the anionic surfactants. This type of variation is also found in presence of increasing mole fraction of hydrotropes [47].

Rewriting equation 6.3 for ideal conditions (with changed notations for CTAB and SDBS), which is also called Clint equation [1], we have equation 6.7.

$$\frac{1}{cmc^*} = \frac{\alpha_1}{C_{c.1}^{mic}} + \frac{\alpha_2}{C_{c.2}^{mic}} \qquad (6.7)$$

Where, cmc* is the cmc of the mixed system, α_1 and α_2 are the stoichiometric mole fraction of components (CTAB, 1, and SDBS, 2) in binary mixtures are C_1^{mic} and C_2^{mic} are the cmc's of CTAB and SDBS respectively. The cmc* values obtained from the above equation employing surface tension data are given in the table 6.2 for all the mixtures.

Table 6. 2.
Mole fraction of different surfactants with cmc^*.

X_{CTAB} (α_1)	X_{SDBS} (α_2)	cmc^*
0.2	0.8	1.96
0.4	0.6	1.52
0.6	0.4	1.23
0.8	0.2	1.04

The differences in the experimental values of the cmc and cmc* value shows the deviation from ideality. It is indeed interesting to note that the non-ideality of the CTAB and SDBS mixtures is not large. However, the charge neutralization between the head groups of the two components and the interaction of hydrophobic part of CTAB is the SDBS micelles improve the hydrophobic environment in the mixed state in comparison to the pure state. As a result, cmc's of the mixture is lower compared to that of pure SDBS micelles. While strong non-ideality is usually expected for anionic / cationic mixtures where strong attractive columbic forces exist, the weak non-ideal behaviour shown by present mixture is indeed interesting. To analyse the synergistic effect of mixed surfactant, different methods are mentioned in literature to calculate interaction parameter. Among these methods, Rubingh's regular solution model is often applied [54].

Interaction parameter

Interaction parameters for mixed micelle system have been calculated by applying Rubingh's model [54]. According to this model, α_1, cmc $\left(C_C^{mic}\right)$ and x_1 (mole fraction of component 1, i.e., CTAB) in mixed micelles are related according to the following equation.

$$\frac{[x_1^2\, ln(C_c^{mic}\alpha_1/C_c^{mic}x_1)]}{(1-x_1)^2\, ln[C_c^{mic}(1-\alpha_1)/C_{c.2}^{mic}(1-x_1)]} = 1 \qquad (6.8)$$

The values of x_1 were obtained by solving above equation by successive approximation method. The micelle mole fraction in the ideal state (x_1^{ideal}) has been computed using

$$x_1^{ideal} = \left[\left(\alpha_1 C_{c.2}^{mic}\right)/\left(\alpha_1 C_{c.2}^{mic} + (1-\alpha_1) C_{c.1}^{mic}\right)\right] \qquad (6.9)$$

The miceller molecular interaction parameter (β) is given by the equation:

$$\beta = \frac{\left[ln\left(\frac{C_c^{mic}\alpha_1}{C_{c.1}^{mic}x_1}\right)\right]}{(1-x_1)^2} \qquad (6.10)$$

The β values may vary from negative to positive through zero. This demonstrates the extent of interaction between the two components which leads to the deviation from ideality. Various theoretical methods are available to interpret the formulation of mixed micelles. The final model given by Lange, and used by Clint, is based on the phase separation model and assumes ideal mixing of the surfactants in the miceller phase. Rubingh proposed a treatment based on 'regular solution theory' (RST) for non ideal mixed systems which have been extensively used. The reason for the non-ideal behaviour among surfactant molecules upon mixing are then various types of molecular interactions. These interactions (either synergistic or antagonistic) can be analysed by RST which allows the evaluation of micelle mole fraction (x_1) and interaction parameter (β^m). According to RST, the molecules of mixing components should be of comparable size, completely interchangeable, and the interaction energy could be expressed as seem of pair wise neighbour interactions. The value of β is proportional to the free energy of mixing, a negative β value means synergism in the system. Thus, a negative deviation from ideal behaviour, corresponding to negative β values is believed to result from a net attraction between the two different surfactant molecules. It indicates that the attractive interactions between the two component molecules are stronger than the interaction among molecules of same components. Positive β values have been ascribed to antagonistic behaviour. It means that the repulsive forces between two mixing components are stronger than the repulsions among similar molecules. A β^m value close to zero means the mixing is almost ideal [55].

Table 6.3.
The computed values of x_1 and β parameters for the present mixture of SDBS and CTAB [Interaction Parameters of CTAB/SDBS System (1) CTAB = 1; SDBS = 2)]

α_{CTAB}	α_{SDBS}	cmc(c)[a] (mM)	Cmc[b] (ST) (mM)	cmc (avg) (mM)	X_1	cmc* /mM	β	f_1	f_2
0	1.0	2.78	2.82	2.80	-	2.80	-	-	-
0.2	0.8	1.49	1.40	1.445	0.539	0.9	-2.45	0.175	0.4889
0.4	0.6	1.25	1.25	1.25	0.569	0.9	-0.128	0.916	0.959
0.6	0.4	1.15	1.10	1.125	0.749	0.9	+0.021	1.009	1.0119
0.8	0.2	0.94	0.93	0.935	0.839	0.9	-0.364	0.897	0.773
1.0	0.0	0.90	0.90	0.90	-	0.9	-	-	-

[a] measured from conductivity data; [b] measured from surface tension data.

For anionic and cationic surfactant mixture, β values are usually found to be highly negative. This indicates very strong synergism [56-57]. Significant synergistic effects have been observed for mixtures of two ionic surfactants with identical head groups but different hydrocarbon part [58-59]. It has also been argued that synergistic effects mostly are due to entropy contributions to the aggregation free energy rather than to specific interactions among the surfactant headgroups [55]. In the present system of CTAB and SDBS mixture, β values are also negative as found within the range of -2.45 to -0.364 (table 6.3). Previous results revealed that the free energy of forming a surfactant aggregate can be written as a sum of several contributions [60,61]: (i) the reduction of contact area between hydrocarbon and water, (ii) conformational entropy due to packing restrictions of the hydrocarbon chains, (iii) electrostatics for a charged aggregate surface and its diffuse layer of counterions, (iv) additional contributions related to the head groups, and (v) entropy of mixing the two surfactants. Electrostatics yields a large contribution to the aggregate free energy for mixtures consisting of ionic surfactants. According to the Poisson-Boltzmann (mean field) description, this contributions mainly due to the entropically unfavourable organization of the counterions into a diffuse layer located outside the electrically charged surface of an aggregate, whereas the purely energetic effects usually are much

smaller for surfactants mixtures like CTAB and SDBS which explains comparatively lower interactions parameter.

Rheology of viscoelastic worm-like micelles found in the system containing SDBS and CTAB in Water

Behaviour of some surfactant mixtures under non-Newtonian flow regime

Aqueous mixtures of anionic and cation surfactant have been found to show fundamentally different properties than the corresponding solutions of pure ionic surfactant or mixture of an ionic and a non-ionic surfactant. The spontaneous formation of rather small unilamellar vescicles has been particularly emphasized, although a number of other structures, such as small globular and large worm-like micelles as well as large lamellar sheets have also been observed [62-64].

The most conspicuous property is, however, the usually large reduction in cmc when two oppositely charged surfactants are mixed in an aqueous solvent. Whereas mixtures of an ionic and a non-ionic surfactant normally yield deviation from ideal behaviour corresponding to $-5 < \beta < -1$, and synergistic effects in mixtures of two non-ionic surfactants are even less, experimentally obtained β values for mixtures of an ionic and a cationic surfactant are usually several magnitudes larger [65]. However, the synergistic effects are observed to increase with increasing length of the surfactant tail. Accordingly, β values for $C_nSO_4^-Na^+$/ $C_nTA^+Br^-$ (TA = trimethyl ammonium) mixtures have been found to be $\beta = -25.5$ for $n = 12$, $\beta = -18.5$ ($n = 10$), and $\beta = -10.5$ ($n = 8$) [66-67].

In analogy with the regular mixture theory, β is generally referred to as the interaction parameter and its deviation from zero has frequently been believed to be the result of specific interactions between the surfactant head groups so that it is different between surfactant 1 and 2 compared to between two identical head groups. According to this interpretation the conspicuously large magnitudes of β found for mixtures of most of the oppositely charged surfactants are due to very strong attractive interactions between the aggregated anionic and cationic head groups, and it has been suggested that such interactions may account for the micelle-to-vesicle transition frequently observed in aqueous cationic surfactant mixtures [52].

On the other hand, present system of cationic and anionic surfactant mixtures of CTAB and SDBS neither exhibits very large deviation from ideality nor yield high β values (β value in the present system lie between -0.364 to -2.45). This is indeed interesting. In all probabilities, the unique behaviour of this mixture stems from the very structure of SDBS molecule, where the alkyl chain is present not as linear long hydrocarbon tail but as the branched chain as shown in section 3.4.1 of this thesis. However, on account of wide industrial applications of SDBS surfactant in various fields, the behaviour of CTAB/SDBS mixture is studied in this work to further detail in non-Newtonian flow regime. Viscoelastic properties including dynamic rheology of the system at different temperature have been investigated to understand the microstructural pattern of the mixed micelles. The self-assembly of both CTAB and SDBS individually result in the formation of globular micelles near the respective cmc values. Further, when these cationic and anionic surfactants are mixed together at low concentration, the mixture synergistically leads to the formation of globular micelles again under Newtonian flow regime, as has already been discussed. On the other hand, when the concentrations of the individual component of the mixtures are increased (e.g., CTAB = 100 mM and SDBS = 20 mM), a viscoelastic gel is formed and the flow becomes non-Newtonian in nature. The observed viscoelasticity is related to worm-like micelle (WLM) formation. The structures of WLM have fascinated scientists because they are similar to polymer chain in their ability to entangle into viscoelastic networks. At the same time, micellar chains are held by weak physical bonds unlike the covalent bonds in polymer; consequently, the chain can break and recombine, and their contour length is not fixed by chemical synthesis but by solution thermodynamics [13]. From a rheological standpoint, wormlike micellar samples are interesting because they can behave as Maxwell fluids (i.e., as model viscoelastic fluids having just a single relaxation time) [68].

Therefore, in general, the experimental solutions exhibit three regions of rheological response. First, at low surfactant concentration, the solutions are Newtonian liquids with low viscosity and non-measurable elastic response. Second, with increasing surfactant concentration, they behave like polymer solutions in the semi-dilute regime, characterized by viscoelastic behaviour with a spectrum of relaxation times. Finally, with increase in the counter ion concentration, these materials enter a regime where their rheological response is similar to that of an entangled polymer or weak gel; however, unlike polymer systems, there relaxation

after shear is dominated by a single relaxation time. In the present chapter of the thesis rheology of viscoelastic worm-like micelles formed in the system of SDBS and CTAB mixtures have been studied.

Rheology of worm-like micelles formed in SDBS and CTAB system

Modelling techniques are used to quantify rheological parameters that can be obtained from oscillating shear results. Many authors have used simple Maxwell element to fit rheological data obtained from viscoelastic surfactant solutions [69-70]. A simple Maxwell element describes the rheological behaviour of a system as a single spring connected in series to a viscous element (dashpot). In shear experiments, this results in equations from G' and G'' of the form

$$G'(\omega) = \frac{G_N^0 \omega^2 \tau^2}{1+\omega^2\tau^2} \qquad (6.11)$$

$$G''(\omega) = \frac{G_N^0 \omega \tau}{1+\omega^2\tau^2} \qquad (6.12)$$

Where G' and G'' are elastic modulus and viscous modulus respectively, ω is the frequency, G_N^0 is the plateau modulus, and τ is the relaxation time. In the time domain, this type of model has single exponential decay, with $G(t) = G_N^0 e^{-t/\tau}$. Maxwell elements are useful in determining G_N^0 and τ of systems dominated by a single relaxation time or in a limited portion of a materials frequency response range if the relaxation times are well separated.

In our experiments, the rheological data are typical of viscoelastic wormlike micelles, with a plateau in G' at high frequencies and terminal behaviour of G' and G'' at low frequencies [figure 6.14 to 6.23]. Moreover, the sample is nearly a Maxwell fluid over a short range of temperatures (303 K - 335 K). Plots are shown from temperature range 273 to 313 K. No cross over point is displayed beyond the temperature range of 303 K - 313 K, except at 281 K. We find that the Maxwell model fits the data well, especially at low and intermediate frequencies, as has been shown for normal worm in the above temperature ranges. Turning to the effect of temperature on the rheological data, we have also found that as the temperature increases, the entire frequencies move or shorter time scales, but the plateau modulus G_p remains constant which was also reported by several workers in other systems [69-71]. This shift in crossover frequency to higher values means that the relaxation time decreases with temperature.

Mukherjee [54] had proposed that an additive which is surface active to a hydrocarbon-water interface will be mainly solubilized at the head group region and will promote micelle growth. Therefore, CTAB is expected to be embedded between SDBS monomers of the micelles. This embedding of CTAB may increase the volume of the micelle. This consequently modify the effective spontaneous curvature via modified packing parameter is responsible for the micelle growth in one dimension. The result is the micro-structural transformation from spherical to wormlike micelle with increasing CTAB concentrations in presence of SDBS. When micelles are sufficiently long, they are converted into more flexible wormlike micelles which can flow comparatively easily. Which reflects by a level off in the G'. At further high concentration, a micro-structural change in micelle structure results the change in rheological parameter. The increase in viscosity to a very small extent can be attributed also by micro-structural change. It is expected that a sufficient amount of CTAB will be present which will embedded between the head groups. Further with increase in temperature, the Br^- ion may be released and would show higher preference for the bulk phase. Such a release if occurs would increase the effective head group area, thereby driving micro-structural change of higher curvature resulting in an increase in viscosity.

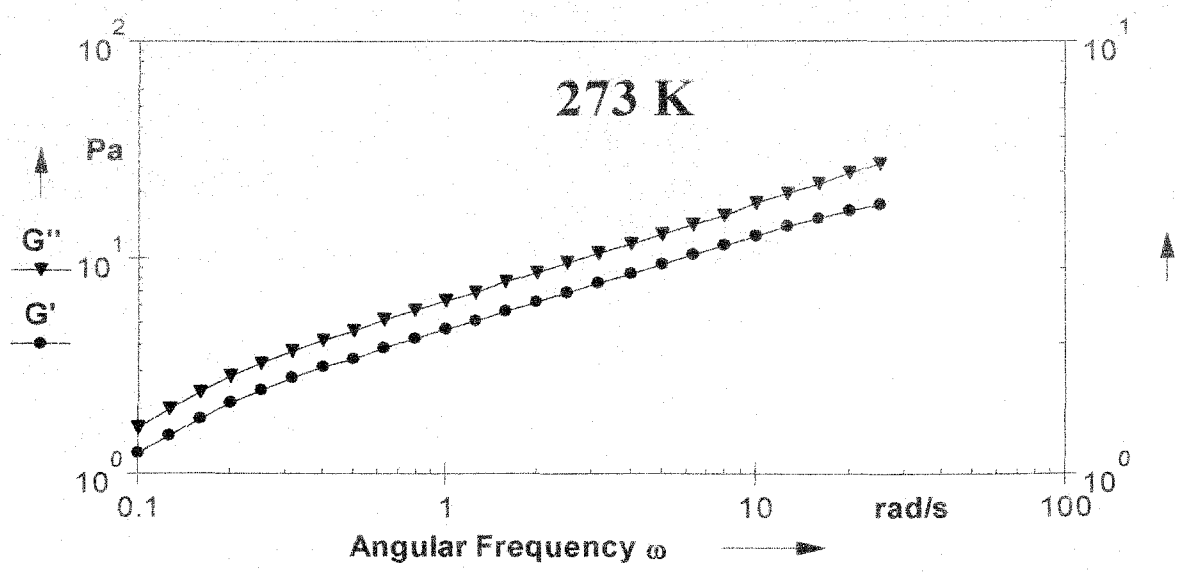

Figure 6.14: Steady shear frequency curves of CTAB and SDBS mixture [CTAB (100 mM) + SDBS (20 mM)]: variation of G′, G″ with angular frequency (temperature = 2° C or 275 K); crossover frequency, ω = not within inspected range; complex viscosity, η^* = 20.443 Pa.s; strain, Υ = 10 %)

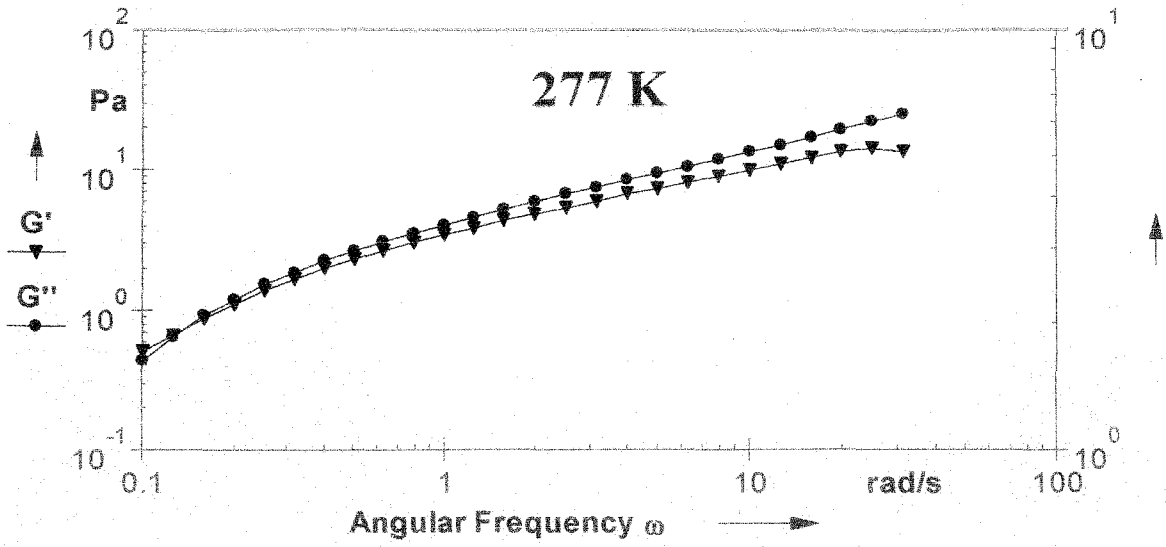

Figure 6.15: Steady shear freequency curves of CTAB and SDBS mixture [CTAB (100 mM) + SDBS (20 mM)]: variation of G′, G″ with angular frequency (temperature = 4° C or 277 K); crossover frequency, ω = not within inspected range; complex viscosity, η^* = 7.648 Pa.s; strain, Υ = 10 %).

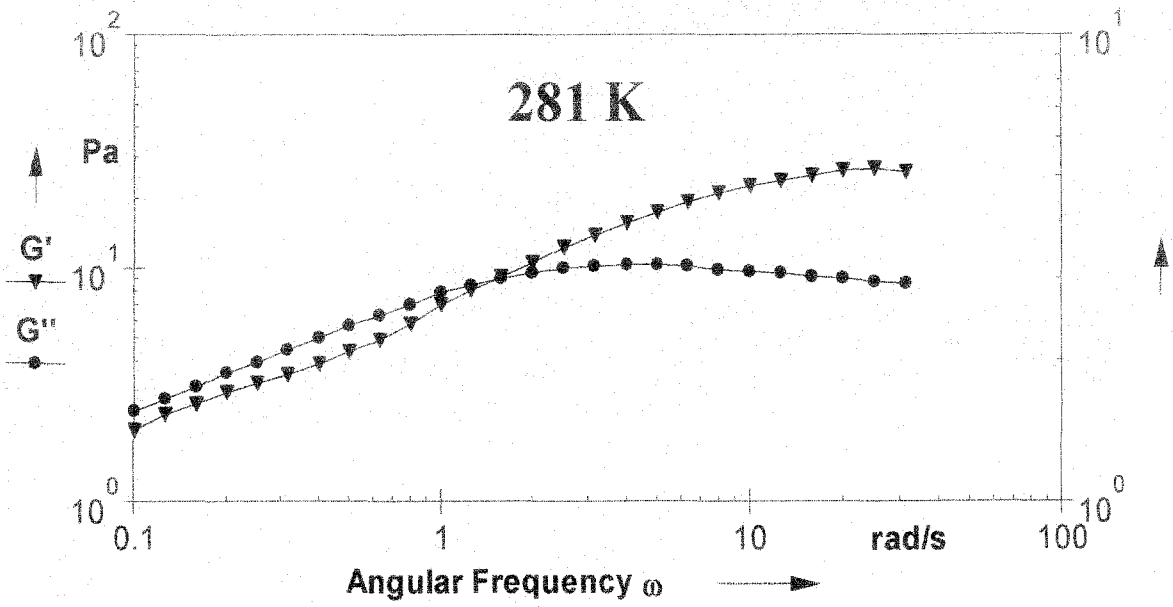

Figure 6.16: Steady shear frequency curves of CTAB and SDBS mixture [CTAB (100 mM) + SDBS (20 mM)]: variation of G′, G″ with angular frequency (temperature = 8° C or 281 K); crossover frequency, ω = 1.499 rad.s^{-1}; complex viscosity, η^* = 68.825 Pa.s; strain, Υ = 10 %).

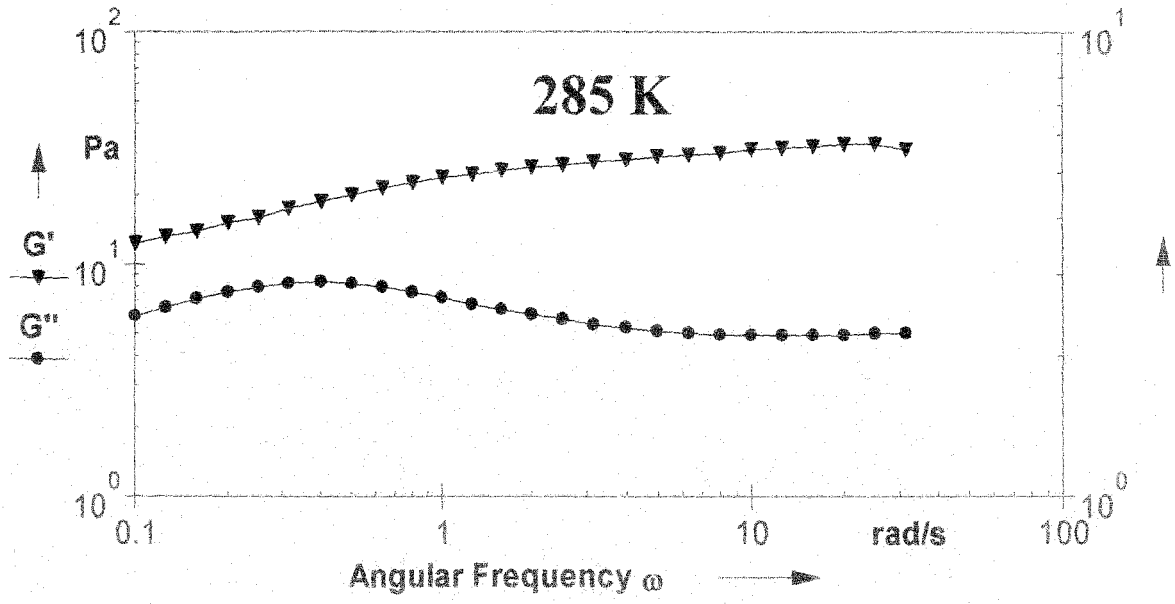

Figure 6.17: Steady shear freequency curves of CTAB and SDBS mixture [CTAB (100 mM) + SDBS (20 mM)]: variation of G′, G″ with angular frequency (temperature = 12⁰ C or 285 K); crossover frequency, ω = not within inspected range; complex viscosity, η^* = 258.5 Pa.s; strain, Υ = 10 %).

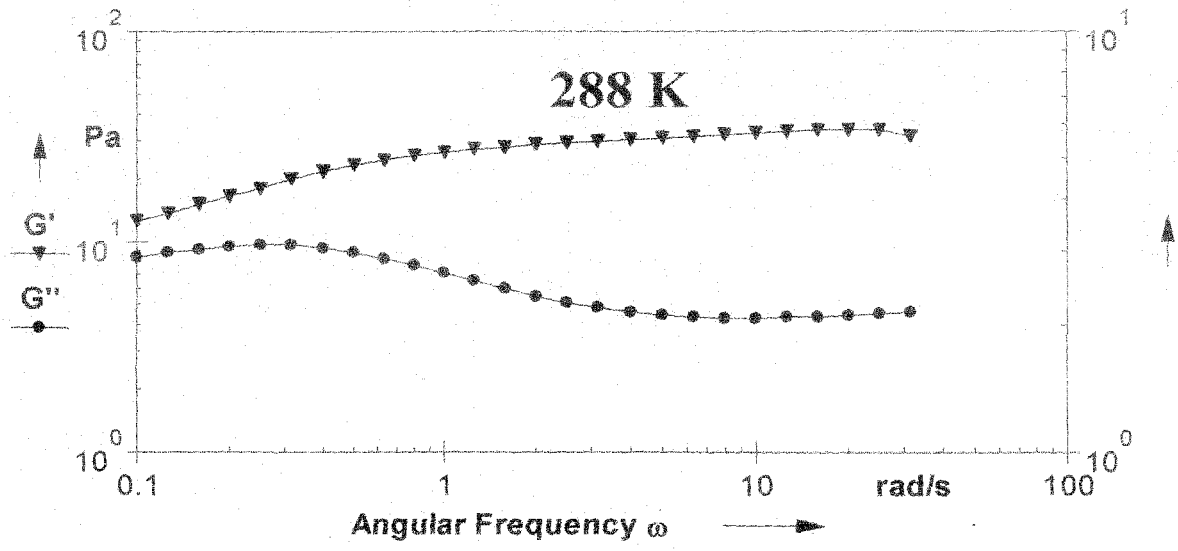

Figure 6.18: Steady shear freequency curves of CTAB and SDBS mixture [CTAB (100 mM) + SDBS (20 mM)]: variation of G′, G″ with angular frequency (temperature = 15⁰ C or 288 K); crossover frequency, ω = not within inspected range; complex viscosity, η^* = 253.36 Pa.s; strain, Υ = 10 %).

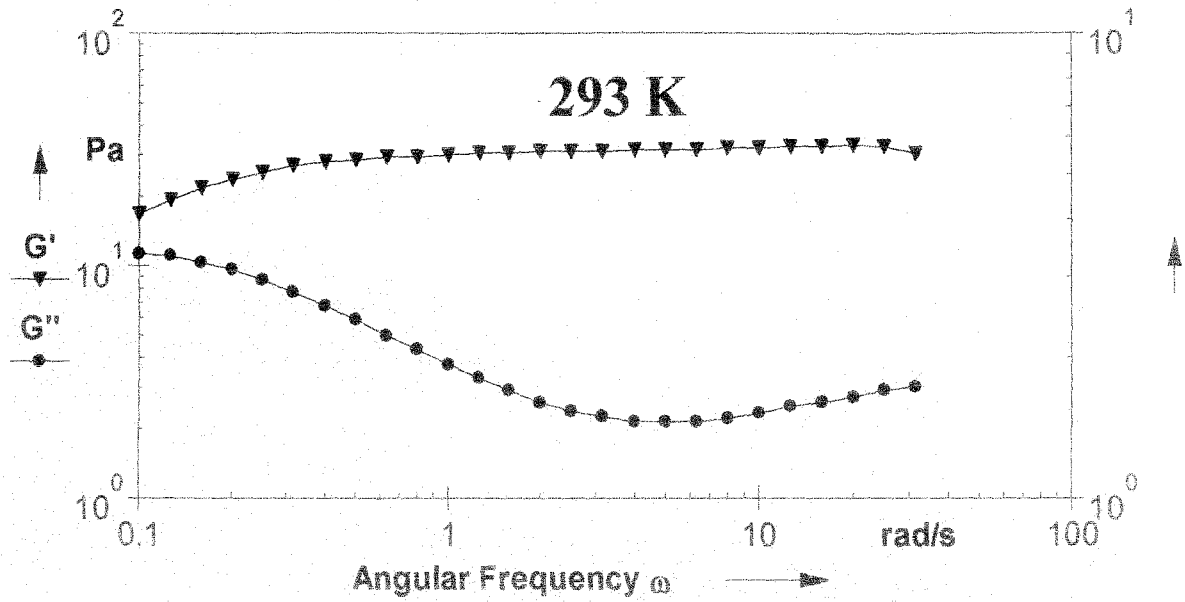

Figure 6.19: Steady shear frequency curves of CTAB and SDBS mixture [CTAB (100 mM) + SDBS (20 mM)]: variation of G′, G″ with angular frequency (temperature = 20° C or 293 K); crossover frequency, ω = not within inspected range; complex viscosity, η^* = 247.65 Pa.s; strain, Υ = 10 %).

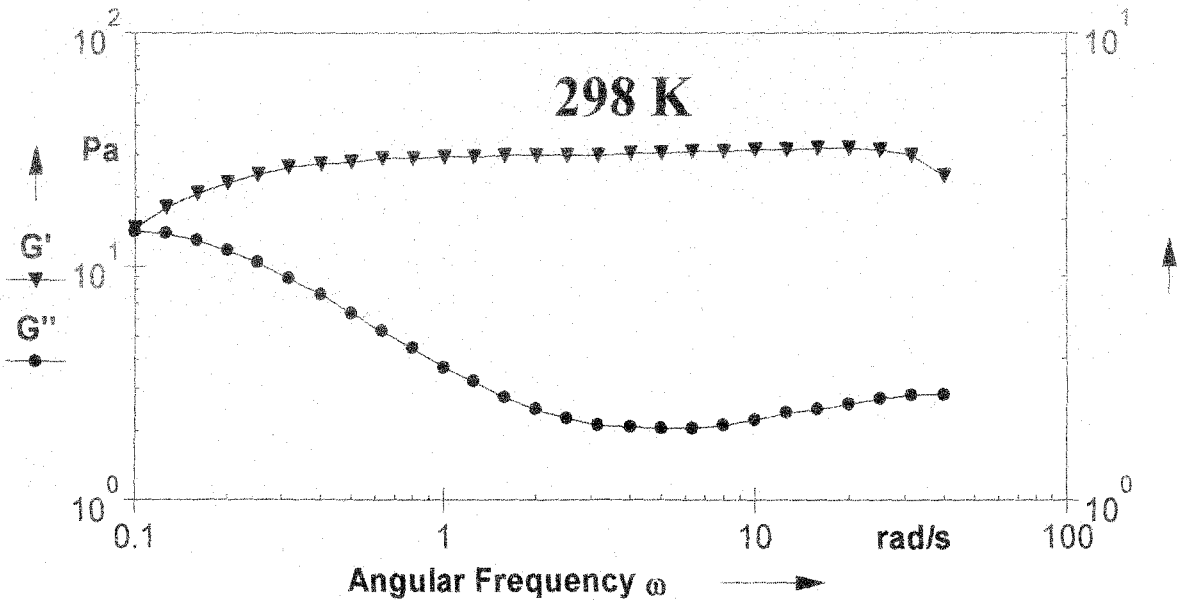

Figure 6.20: Steady shear frequency curves of CTAB and SDBS mixture [CTAB (100 mM) + SDBS (20 mM)]: variation of G′, G″ with angular frequency (temperature = 20° C or 298 K); crossover frequency, ω = not within inspected range; complex viscosity, η^* = 232.75 Pa.s; strain, Υ = 10 %).

A representative fitting of Maxwell model is shown, which indicates fairly good fitting at low frequencies.

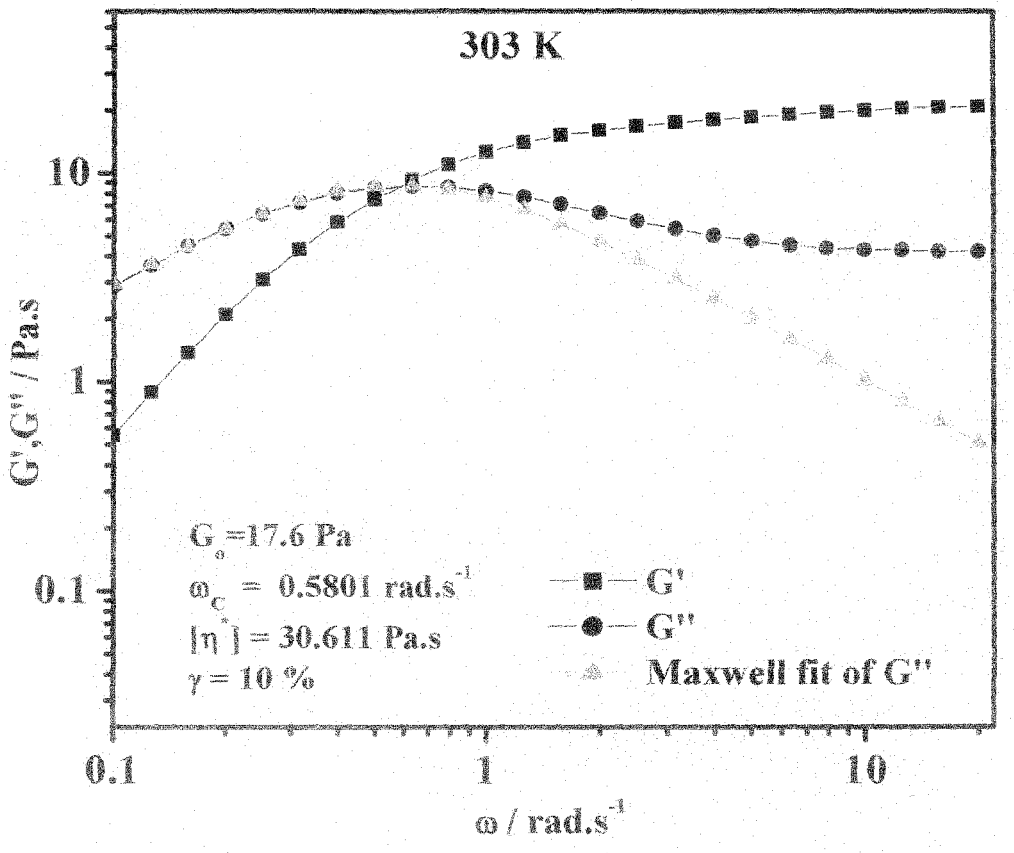

Figure 6.21: Steady shear frequency curves of CTAB and SDBS mixture [CTAB (100 mM) + SDBS (20 mM)]: variation of G', G'' with angular frequency (temperature = 30°C or 303 K); crossover frequency, $\omega = \omega_c = 0.5801$ rad.s^{-1}; complex viscosity, $\eta^* = 30.611$ Pa.s; strain, $\gamma = 10\%$).

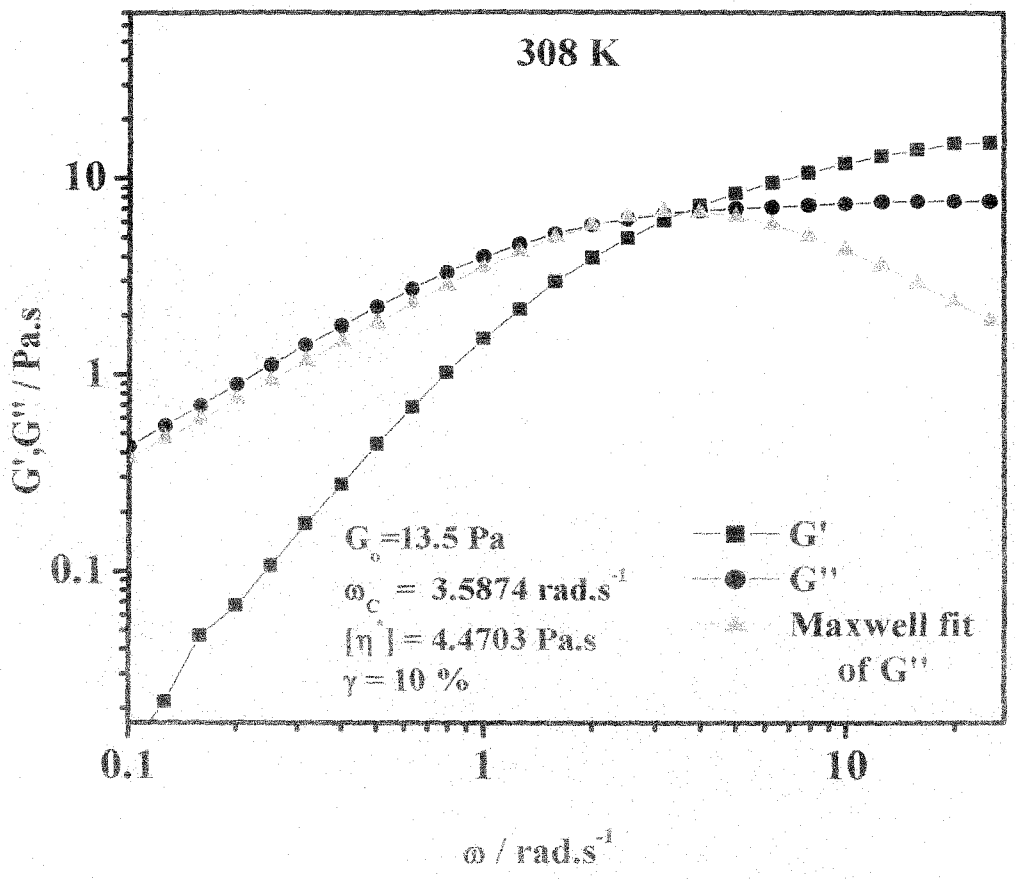

Figure 6.22: Steady shear frequency curves of CTAB and SDBS mixture [CTAB (100 mM) + SDBS (20 mM)]: variation of G′, G″ with angular frequency (temperature = 35°C or 308 K); crossover frequency, $\omega = \omega_c = 3.5874$ rad.s^{-1}; complex viscosity, $\eta^* = 4.4703$ Pa.s; strain, $\gamma = 10\%$).

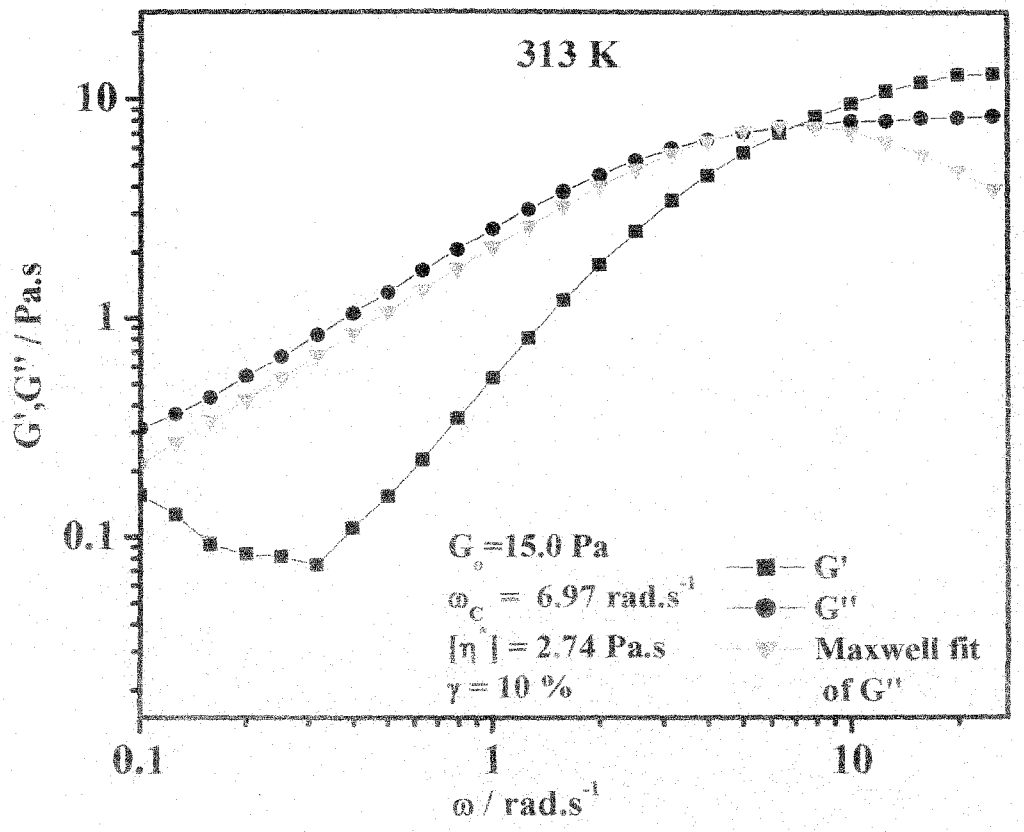

Figure 6.23: Steady shear frequency curves of CTAB and SDBS mixture [CTAB (100 mM) + SDBS (20 mM)]: variation of G', G'' with angular frequency (temperature = 40° C or 313 K); crossover frequency, $\omega = \omega_c = 6.9719$ rad.s^{-1}; complex viscosity, $\eta^* = 2.7426$ Pa.s; strain, Y = 10%).

From the oscillatory rheometry figures 6.14 to 6.23, there is clear viscoelastic behaviour of certain SDBS and CTAB mixtures. At low frequencies the loss modulus (G'') is higher than the storage modulus (G'), indicating that the sample behaves as a liquid and also predominantly viscous whereas at high freequencies, G' is greater than G'', which implies that the mixtures behave like a solid which is predominantly elastic in the temperature range 303 – 313 K. As has already been mentioned that the data fits to the Maxwell model of relaxation at low freequencies but diverges at high freequencies, which is typical of worm like micellar solution with several relaxation modes [72]. The dip of the G'' curve even at higher freequencies is due to the presence of further relaxation modes.

It is sometimes difficult to determine how "good" a Maxwell model fits the data from plots of G' and G'' versus ω. Systems that have a spectrum of closely spaced relaxation times may appear to be fit by a single Maxwell's element. Cole - Cole or Nyquist plots (plots of G'' as a function of G') provide a better picture of how well this data correspond to a single relaxation time Maxwell model. A Cole - Cole plot for a perfect Maxwell element is a semicircular, where as a plot for a system with many relaxation times in a narrow range is boxlike. The curve in the present system fits to good extent to a simple Maxwell model (figure 6.24 - 6.26). The data points fit fairly well on a semicircle curve particularly at 303 K. A single exponential relaxation can be effectively explained in case of worm like micelles. According to Cates, the possibility of breaking and recombination introduces new mechanism for stress relaxation for living polymers, in addition to the raptation process [72]. Mean filled model introduces two characteristic times for this process, these are raptation time of an unbreakable chain and the average time before such a chain breaks into two pieces as a result of the reversible scission process. Several theories have been predicted depending on the relative ratio of the two characteristics time scales. From these theories, it may be concluded that when average time is very much greater than the reputation time, the micelles behave like ordinary polydisperse unbreakable polymers with exponential polydispersity and the stress relaxation function which are different from monodisperse polymers. When reputation time is greater than average time, chain breakage and recombination will both occur often for a typical chain, before it has disengaged from the tube by ordinary reputation. In this case, the reputation mechanism is short circuited and the new relaxation process will be monoexponential with a new time scale. This explains the observed single exponential behaviour of the system, because before a given tube segment relaxes, the chain occupying it typically undergoes many scission and recombination reactions, so that there is no memory of either the initial length of the chain or the position on the chain initially corresponding to the tube segment. The deviations from the half circle occur at a circular frequency ω of the order of the inverse of the breaking time of the micelles. At higher frequencies the data deviate from the Maxwell model, which is typically the case when the systems can no longer be described by a single relaxation time. So, a Cole - Cole plot can easily visualize how well the data correspond to the Maxwell model. The large deviation from Cole - Cole plot with high angular viscosity is indicative that of a less structured system with poor viscoelastic behaviour.

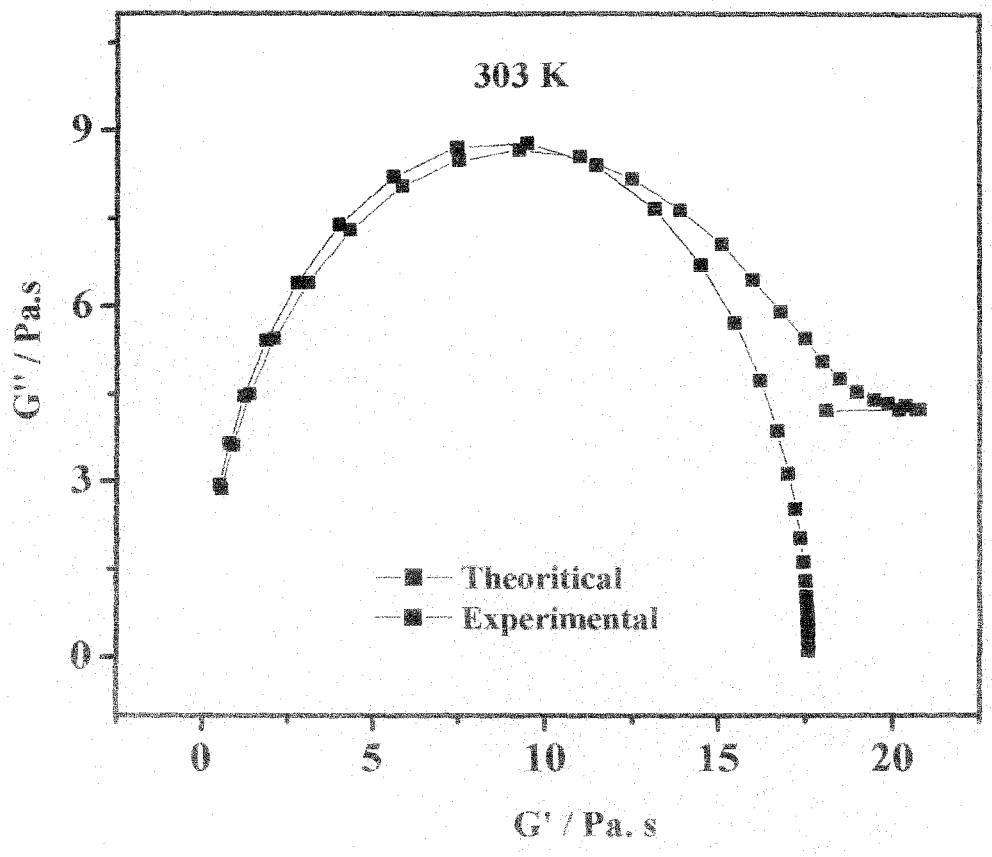

Figure 6.24: Cole – Cole Plot (G'' as a function of G') using data presented in figure 6.23 at 303 K.

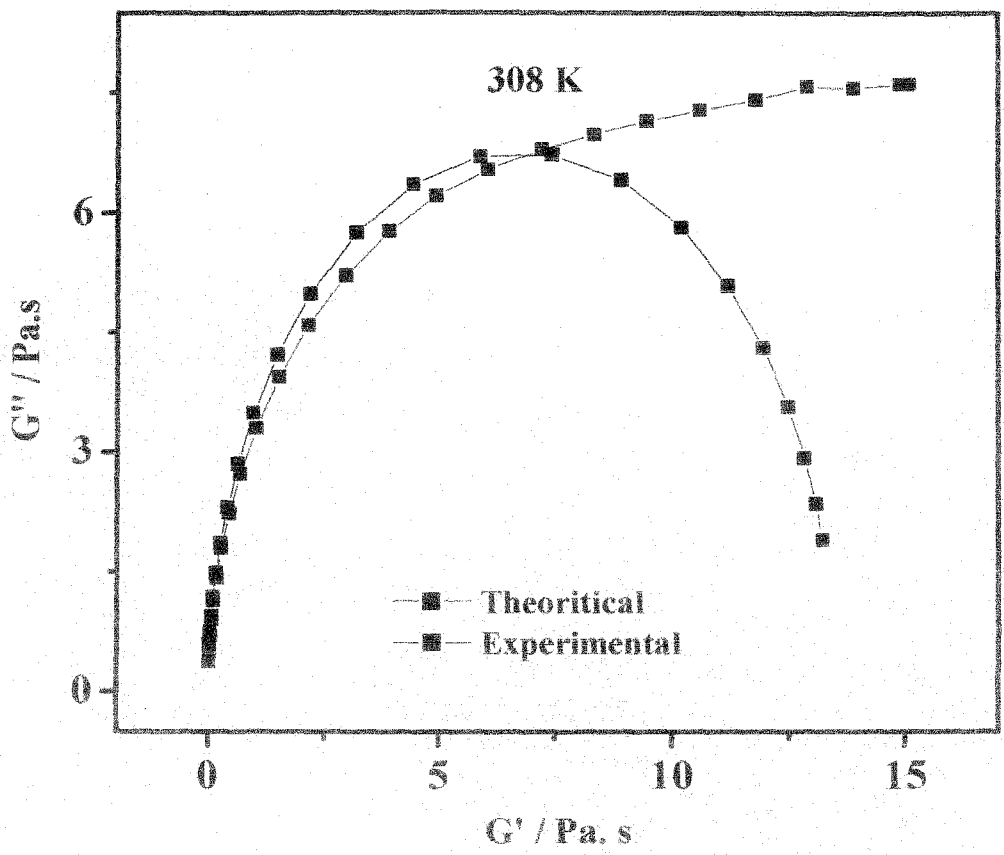

Figure 6.25: Cole – Cole Plot (G'' as a function of G') using data presented in figure 6.24 at 308 K.

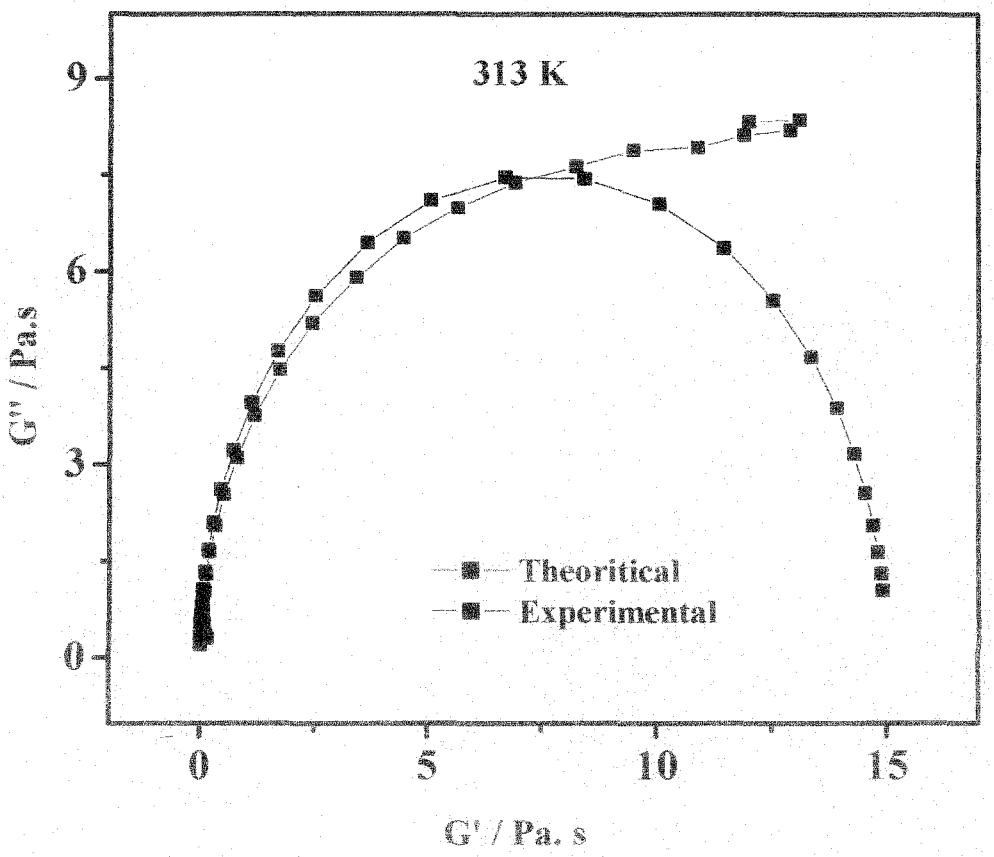

Figure 6.26: Cole – Cole Plot (G'' as a function of G') using data presented in figure 6.25 at 313 K.

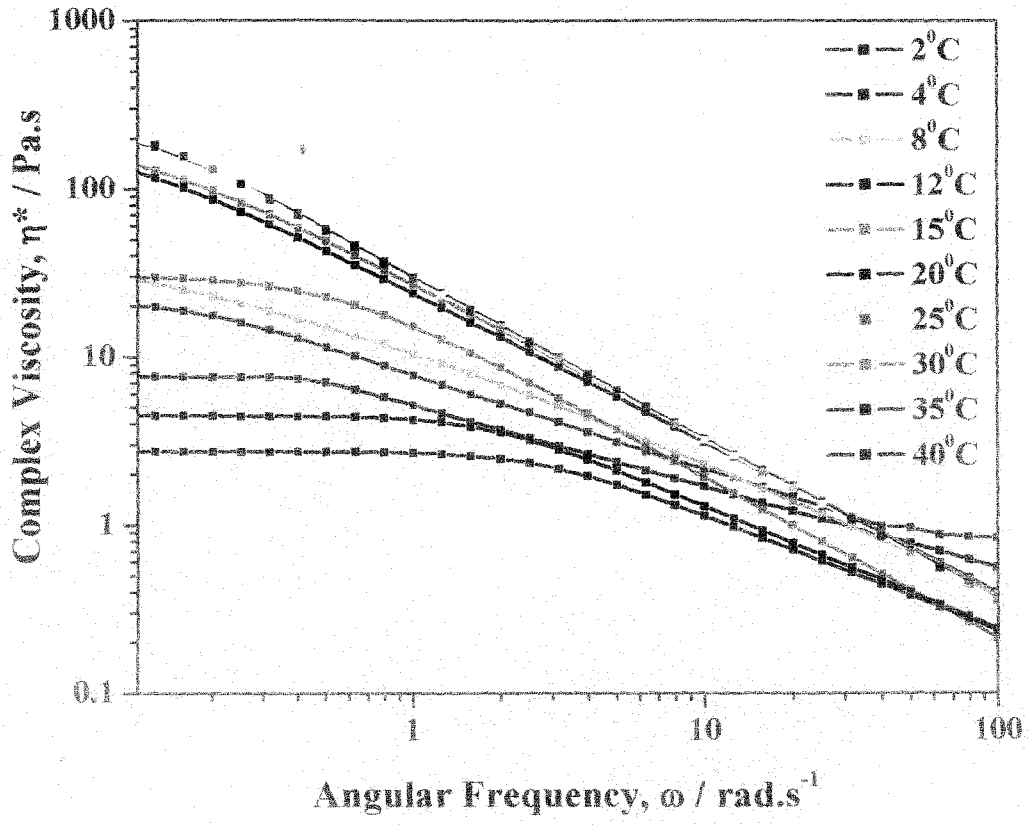

Figure 6.27: Complex viscosity Vs. Angular frequency plot

It is noteworthy that for the present surfactant mixtures the experimental data for G' and G'' deviate from the Maxwell model at higher freequencies. Granek and Cates have shown that the high freequency deviations can be accounted for by the Rouse models and the primitive path fluctuations along the micelle chain [23]. Similar results were also obtained for other viscoelastic samples in the higher concentration range [73-74].

The zero-shear viscosity of the surfactant mixtures was determined from controlled-stress measurements by extrapolating the viscosity-shear stress curve to zero shear rate.

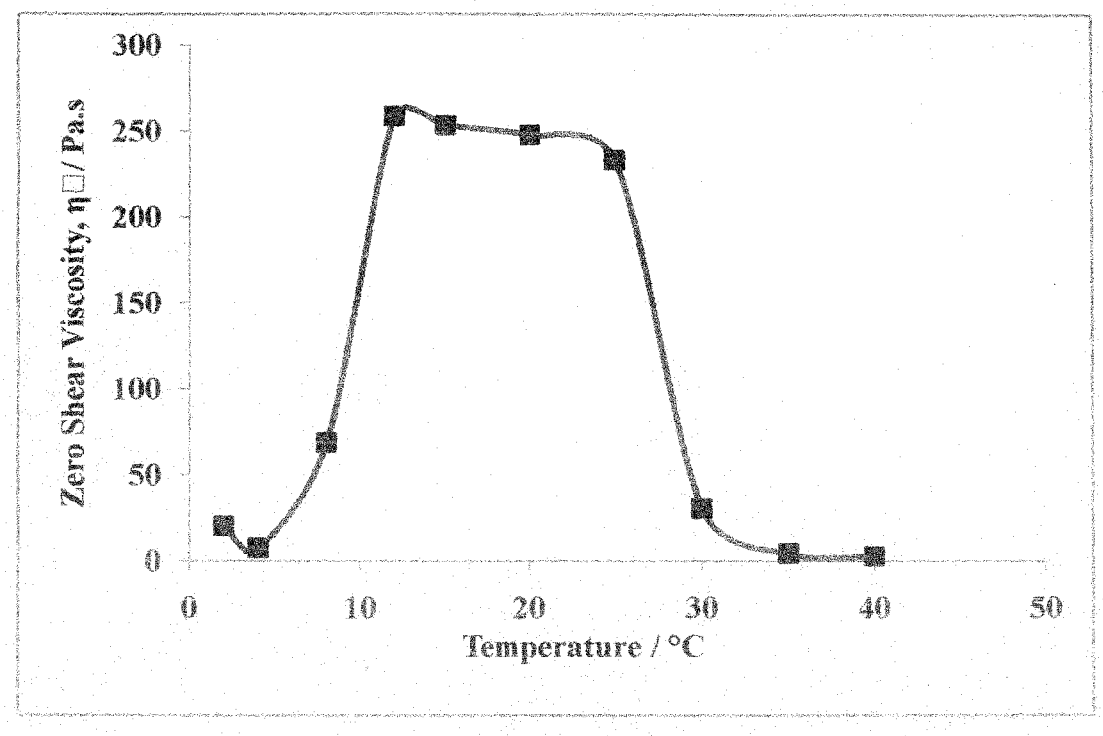

Figure 6.28: Variation of Zero Shear Viscosity, η_0 with Temperature of the surfactant mixture {CTAB (100 mM) + SDBS (20 mM)}.

In terms of stress relaxation, it is slowest at the viscosity peak and increases at both lower and higher temperatures. Figure 6.28 shows the change in η_0 with temperature. It is clear that with increase in temperature, η_0 increases indicating an increase in the curvature energy for surfactant aggregates which leads to an increase in micellar length and the formation of wormlike micelles. As the temperature further increased, the zero shear viscosity exhibits a flat maximum within 10°C to 26°C temperatures. Further increase in temperature decreases the zero shear viscosity can be explained as a decrease of the micellar contour length or the formation of branched micelles as also found by other researchers [78]. In summary, all these results support a fascinating and complex rheology to exist in the present system is a structural evolution from a spherical micelle to a worm like micelle.

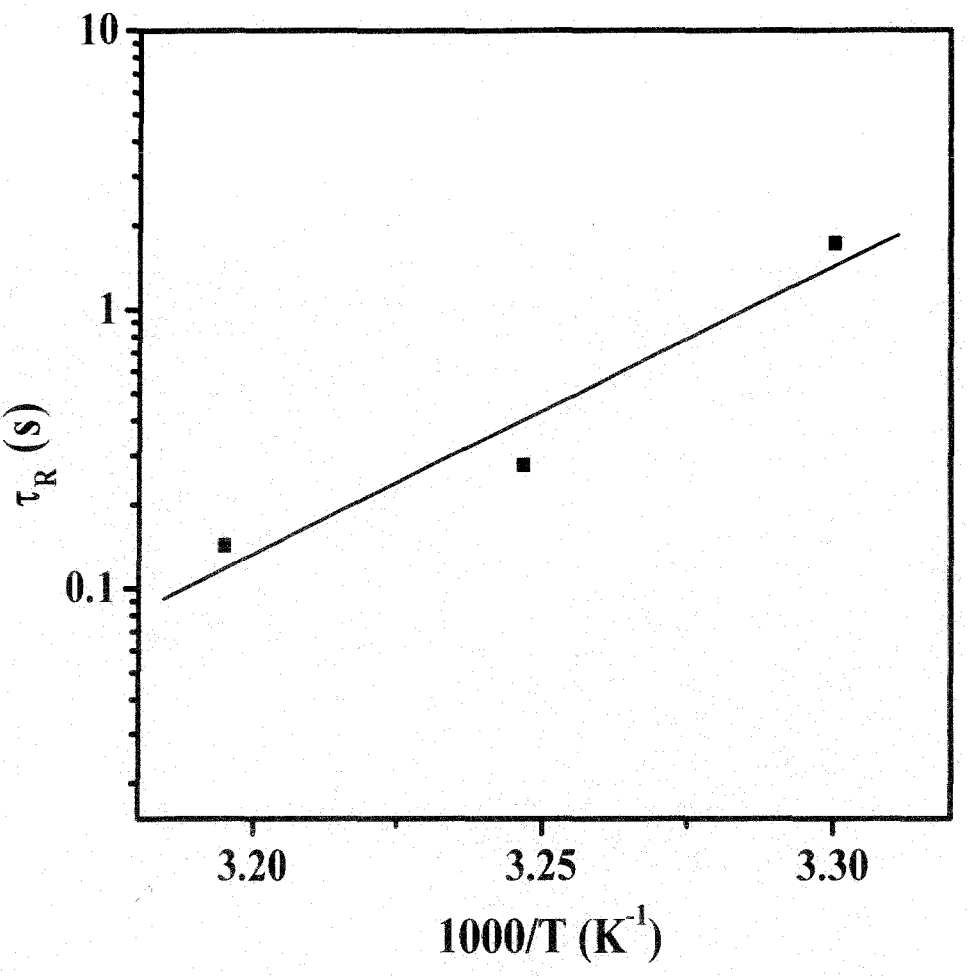

Figure 6.29: Arrhenius Semi log plot of τ_R vs 1/T for CTAB-SDBS (100 mM: 80 mM) system .

Finally, the shift in cross over freequency ω to higher values indicate that the relaxation time τ decreases with temperature (figure 6.22-6.24). The variation of τ with temperature is shown in figure 6.31 on Arrhenius plot (i.e., a semilog plot of the quantities vs. 1/T). We find that the τ values fall on a straight line, indicating an exponential decrease that can be represented by the following equation.

$$\tau = A \exp\left(\frac{E_A}{RT}\right) \qquad (6.13)$$

Where E_A is the flow activation energy, R is the gas constant, T is the absolute temperature and A is the pre exponential factor. The figure shows that for the present system containing CTAB and SDBS mixture, the E_A value is 85.44 kJ/mol, which is comparable with represented values for other similar systems.

References:

1. J. M. Lehn, *Science*, **2002**, 295, 2400

2. G. M. Whitesides and M. Boncheva, *Proc. Natl. Acad. Sci. U. S. A.*, **2002**, 99, 4769.

3. D. Philip and J. F. Stoddart, *Angew. Chem., Int. Ed. Engl.*, **1996**, 35, 1155.

4. H. W. Jun, S. E. Paramonov and J. D. Hartgerink, *Soft Matter*, **2006**, 2, 177.

5. T. J. Deming, *Soft Matter*, **2005**, 1, 28.

6. Y. Lin, Y. Qiao, Y. Yan and J. Huang, *Soft Matter*, **2009**, 5, 3047.

7. Fuhrhop, J - H and Helfrich. W., *Chem. Rev.*, **1993**, 93, 1565 - 1582.

8. Salkar, R. A., Hassan, P. A., Samant, S. D., Valaulikar, B. S., Kuma, R. V. V., Kern, F., Candau, S. J. and Manohar, C., *J. Chem. Soc., Chem. Comm.*, **1996**, 1223 - 1224.

9. S. Svenson, *Curr. Opin. Colloid Interface Sci.*, 2004, 9, 201

10. T. Kunitake and Y. Okahata, *J. Am. Chem. Soc.*, **1977**, 99, 3860.

11. J. C. Hao and H. Hoffmann, *Curr. Opin. Colloid Interface Sci.*, **2004**, 9, 279.

12. S. J. Candau, E. Hirsch and R. Zana, *J. Colloid Interface Sci.*, **1985**, 105, 521.

13. M. E. Cates and S. J. Candau, *J. Phys.: Condens. Matter*, **1990**, 2, 6869.

14. M. E. Cates, *J. Phys. Chem.*, **1990**, 94, 371.

15. S. J. Candau, A. Khatory, F. Lequeux and F. Kern, *J. Phys. IV*, **1993**, 3, 197.

16. E. J. Magid, *J. Phys. Chem. B*, **1998**, 102, 4064.

17. C. A. Dreiss, *Soft Matter*, **2007**, 3, 956.

18. S. Ezrahi, E. Tuval and A. Aserin, *Adv. Colloid Interface Sci.*, **2006**, 128, 77.

19. H. Rehage and H. Hoffmann, *Mol. Phys.*, **1991**, 74, 933.

20. Bandyopadhyay, R., Basappa, G and Sood, A. K., *Phys. Rev. Lett.*, **2000**, 84, 2022.

21. Ganapathy, R.; Sood, A. K. and Ramaswamy, S. *EPL*, **2007**, 77, 18007.

22. Granek, R., Cates, M. E., *J. Chem. Phys.*, **1992**, 96, 4758 - 4767.

23. Torres, M.F.; Gonzalez, J. M.; Rojas, M.R.; Muller, A. J.; Saez, A. E.; Lof. D.; Schillen, K. *J. Colloid Interface Sci.* **2007**, 307, 221 - 228.

24. Mishic, J. R.; Fisch, M. R., *J. Chem. Phys.* **1990**, 92, 3222 - 3229.

25. Lin, Z.; Cai, J.; Scriven, L. E.; Davis, H. T., *J. Phys. Chem.* **1994**, 98, 5984 - 5993.

26. L. M. Walker, *Curr. Opin. Colloid Interface Sci.*, **2001**, 6, 451.

27. G. C. Maitland, *Curr. Opin. Colloid Interface Sci.*, **2000**, 5, 301.

29. J. Yang, *Curr. Opin. Colloid Interface Sci.*, **2002**, 7, 276.

29. J. L. Zakin and H. W. Bewersdorff, *Rev. Chem. Eng.*, **1998**, 14, 2533.

30. R. D. Koehler, S. R. Raghavan and E. W. Kaler, *J. Phys. Chem. B*, **2000**, 104, 11035.

31. S. R. Raghavan, G. Fritz and E. W. Kaler, *Langmuir*, **2002**, 18, 3797.

32. B. A. Schubert, E. W. Kaler and N. J. Wagner, *Langmuir*, **2003**, 19, 4079.

33. A Bernheim-Groswasser, E. Wachtel and Y. Talmon, *Langmuir*, **2000**, 16, 4131.

34. K. Imanishi, Y. Einaga, *J. Phys. Chem. B*, **2007**, 111, 62.

35. D. P. Acharya, S. C. Sharma, C. Rodriguez-Abreu and K. Aramaki, *J. Phys. Chem. B.*, **2006**, 41, 20224.

36. H. Hoffmann, A. Rauschera, M. Gradzielski, S. F. Schulz, *Langmuir*, **1992**, 8, 2140.

37. P. Fischer, H. Rehage and B. Gruning, *J. Phys. Chem. B*, **2002**, 106, 11041.

38. R. Kumar, G. Kalur, L. Ziserman, D. Danino and S. Raghavan, *Langmuir*, **2007**, 23, 12849.

39. P. A. Hassan, S. R. Raghavan, E. W. Kaler, *Langmuir*, **2002**, 18, 2543.

40. S. Imai, T. Shikata, *J. Colloid Interface Sci.*, **2001**, 244, 399.

41. K. Bijma, M. J. Blandamer, J.B.F.N. Engberts, *Langmuir*, **1997**, 13, 4843.

42. C. Oelschlaeger, G. Watson, S. J. Candau, *Langmuir*, **2003**, 19, 10495.

43. R. Abdel-Rahem, M. Gradzieski, H. Hoffmann, *J. Colloid Interface Sci.*, **2005**, 288, 570.

46. A. M. Ketner, R. Kumar, T. S. Davies, P. W. Elder and S. R. Raghavan, *J. Am. Chem. Soc.*, **2007**, 129, 1553.

45. Hassan, P. A., Narayanan, J., Manohar, C., *Curr. Sci.*, **2001**, 80, 8, 980.

46. Horbaschek, K., Hoffmann, H. and Thunig, C., *J. Colloid. Int. Sci.*, **1998**, 206, 439-456.

47. Khan, I. A.; Khanam, A. J.; Khan, Z. A.; Kabir-ud-Din, *J. Chem. Eng. Data.*, **2010**, 55, 4775 - 4779.

48. Andelman, D., Kozlov, M. M. and Helfriich, W. *Europhys. Lett.*, **1994**, 25, 231 - 236.

49. Fattal, D. R., Andelman, D. and Ben-Shaul, A. *Langmuir*, **1995**, 11, 1154 - 1161.

50. Kozlov, M. M., Lichtenberg, D. and Andelman, D. *J. Phys. Chem.*, **1997**, 101, 6600 – 6606.

51. Menon, S. V. G., Manohar, C. and Lequeux, F., *Chem. Phys. Lett.*, **1996**, 263, 727 – 732.

52. Salkar, R. A., Mukesh, D., Samant, S. D. and Manohar, C., *Langmuir*, **1998**, 14, 3778 – 3782.

53. Zemb, T., Dubois, M., Deme, B. and Gulikkrzywicki, T. , *Science*, **1999**, 283, 816 – 819.

54. Mukherjee, P.; Mittal, K. L. Solution Chemistry of Surfactants, *Plenum Press*, New York, **1979**.

55. Bergstrom, M. and Eriksson, J. C., *Langmuir*, **2000**, 16, 7173 – 7181.

56. Holland, P. M. *Mixed Surfactant Systems*, Chapter 2, **1992**, pp 40.

57. Jonsson, B.; Lindman, B.; Holmberg, K.; Kronberg, B. *Surfactant and Polymers in Aqueous Solution*, Wiley, Chichester, **1998**, Chapter 5.

58. Garcia-Mateos, I.; Velazquez, M. M.; Rodriguez, L. J. *Langmuir*, **1990**, 6, 1078.

59. Lopez-Fontan, J. L.; Suarez, M. J.; Mosquera, V.; Sarmiento, F. *Phys. Chem. Chem. Phys.* **1999**, 1, 3583.

60. Eriksson, J. C.; Ljunggren, S.; Henriksson, U. *J. Chem. Soc., Faraday Trans. 2*, **1985**, 81, 833

61. Eriksson, J. C.; Ljunggren, S.; *J. Chem. Soc., Faraday Trans. 2*, **1985**, 81, 1209.

62. Kamenka, N.; Chorro, M.; Talmon, Y.; Zana, R. *Colloid Surf.* **1992**, 67, 213.

63. Kaler, E. W.; Herrington, K. L.; Murthy, A. K.; Zasadzinski, J. A. N. *J. Phys. Chem.* **1992**, 96, 6698.

64. Bergström, M.; Pedersen, J. S. *J. Phys. Chem.* B, **2000**, 104, 4155.

65. Holland, P. M. *In Mixed Surfactant systems*, Holland, P. M.; Rubingh, D. N. Eds.; ACS Symposium Series 501; ACS, Washington DC; **1992**, Chapter 2, p 40.

66. Zhu, B. Y.; Rosen, M. J. *J. Colloid Interface Sci.* **1984**, 99, 435.

67. Rosen, M. J. *In Phenomena in Mixed Surfactant Systems*; Scamehorn, J. F., Ed.; ACS Symposium Series 311; ACS, Washington DC, **1986**, p 144.

68. Berret, J. F. *In Molecular Gels*, Weiss, R.G.; Terech, P. Eds. Spinger Dordrecht, The Netherlads, **2005**, p 235.

69. Kem, F.; Zana, R.; Candau, S. J. *Langmuir*, **1991**, 7, 1344.

70. Raghavan, S. R.; Kaler, E. W. *Langmuir*, **2001**, 17, 300.

71. Fischer, P.; Rehage, H. *Langmuir*, **1997**, 13, 7012.

72. Cates, M. E., *Macromolecules*, **1987**, 20, 2289 – 2296.

73. Shrestha, R. G.; Shrestha, L. K.; Matsunga, T.; Shibayama, M.; Aramaki, K. Langmuir, **2011**, 27, 2229.

74. Shrestha,R. G.; Shrestha, L. K.; Aramaki, K. *Colloid. Polym. Sci.* **2009**, 287, 1305.